catalysts

MDPI

Article

Well-Shaped Sulfonic Organosilica Nanotubes with High Activity for Hydrolysis of Cellobiose

Jing Sun [1], Xiao Liu [1,*], Xinli Zhu [1], Hua Wang [1], Sadegh Rostamnia [2,*] and Jinyu Han [1]

[1] Key Laboratory for Green Chemical Technology of Ministry of Education, School of Chemical Engineering and Technology, Tianjin University, Tianjin 300072, China; dugufanying@163.com (J.S.); Xinlizhu@tju.edu.cn (X.Z.); tjuwanghua@tju.edu.cn (H.W.); hanjinyu@tju.edu.cn (J.H.)

[2] Organic and Nano Group (ONG), Department of Chemistry, Faculty of Science, University of Maragheh, Maragheh 55181-83111, Iran

* Correspondence: liuxiao71@tju.edu.cn (X.L.); rostamnia@maragheh.ac.ir (S.R.); Tel.: +86-22-2789-0859 (X.L.); +98-421-2278-001-108 (S.R.)

Academic Editors: Munish Puri and Takuya Tsuzuki
Received: 14 March 2017; Accepted: 19 April 2017; Published: 27 April 2017

Abstract: Sulfonic organosilica nanotubes with different acidity densities could be synthesized through the co-condensation of ethenyl- or phenylene-bridged organosilane and 3-mercaptopropyltrimethoxysilane followed by sulfhydryl (–SH) oxidation. Transmission electron microscopy (TEM) analysis and nitrogen adsorption-desorption experiment clearly exhibit the hollow nanotube structures with the diameters of about 5 nm. The compositions of the nanotube frameworks are confirmed by solid state ^{13}C nuclear magnetic resonance (NMR) while X-ray photoelectron spectroscopy (XPS) shows that about 60–80% of SH groups were oxidized to sulfonic acid (SO_3H). The acid contents were measured by both elemental analysis (CHNS mode) and acid-base titration experiment, which revealed that the acid density was in the range of 0.74 to 4.37 $\mu mol \cdot m^{-2}$ on the solid. These nanotube-based acid catalysts exhibited excellent performances in the hydrolysis of cellobiose with the highest conversion of 92% and glucose selectivity of 96%. In addition, the catalysts could maintain high activity (65% conversion with 92% selectivity) even after six recycles.

Keywords: sulfonic solid acid catalysts; organosilica nanotubes; hydrolysis of cellobiose; acid density

1. Introduction

The preparation of fuels and chemical products derived from biomass is one of the most attractive approaches of the sustainable development for our society [1]. Cellulose, most widely existing in nature as one of the renewable biomass resources, has drawn much attention regarding its efficient utilization [2]. Among the strategies for cellulose utilization, hydrolysis reaction is one of the most important steps. Due to the strong intermolecular and intramolecular hydrogen bonds, traditional acid catalysts including concentrate and diluted sulfuric acids are usually used to realize the cleavage of cellulose [3]. However, such liquid acids are difficult to recycle and reuse, which may cause serious environmental pollution and high production costs [4]. Therefore, considerable efforts have been dedicated to the design and synthesis of effective solid acid catalysts as alternatives.

Organic-inorganic hybrid materials are considered as a kind of novel promising catalyst for the transformation of cellulose, owing to their unique characters such as simple synthetic process, highly stable structures and tunable hydrophilic/hydrophobic properties [5–7]. More recently, periodic mesoporous organosilicas (PMOs) incorporated with different organic moieties have emerged as useful solid catalysts in acid-catalyzed hydrolysis reactions. For example, Van Der Voort et al. synthesized sulfonic acid-functionalized PMOs through a "one-step" method, which can effectively catalyze the esterification of acetic acid and benzyl alcohol [8]. Guo and coworkers inserted

2-(4-chlorosulfonylphenyl)ethyl trimethoxysilane into PMO frameworks formed by two bifunctional organosilanes and the catalysts were evaluated by the esterification of palmitic acid and transesterification of yellow horn seed oil [9]. Such results clearly indicate the big potentials of PMOs incorporated with acid sites in the hydrolysis reactions.

PMOs with nanotube structures have been prepared from bridged organosilane precursors through a simple micelle-templating approach [10]. These nanotubes have distinct advantages such as more active sites, easy access to active sites in the tubes, and confinement effects inside the cavity. Up to now, several kinds of organic groups have been incorporated into the nanotube frameworks, such as ethenyl, phenylene and bipyridine [9,11,12]. Unique properties of these organosilica nanotubes make them be widely used in heterogeneous catalysis, which could reduce the diffusion limitation and facilitate the transport of reactants and products due to the uniform nanotube structures and the large pore diameters [13,14].

Herein, through the co-condensation of organosilica precursors and 3-mercaptopropyltrimethoxysilane under acid conditions in the presence of P123 [$(EO)_{20}(PO)_{70}(EO)_{20}$] as a template agent, we have constructed sulfonic organosilica nanotubes bridged with ethenyl or phenylene in the frameworks, respectively, followed by the sulfhydryl (–SH) oxidation using hydrogen peroxide. These solid nanotube-based acid catalysts showed excellent performances in the hydrolysis of cellobiose (Scheme 1). In addition, in order to investigate the effect of surface acid density, solid catalysts composed of different amount of acidic sites were synthesized. The hydrolysis of cellobiose indicates that improved activity could be achieved with the increasing of acid density.

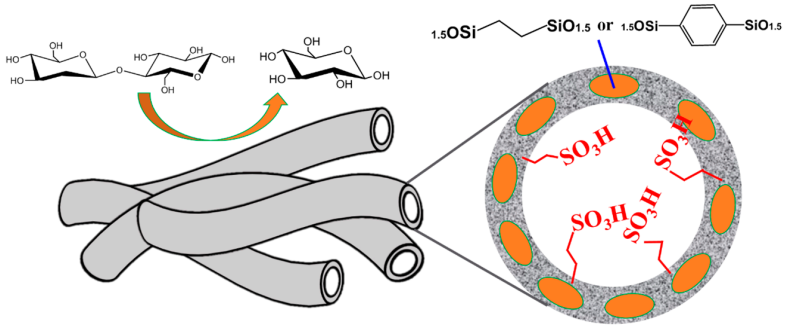

Scheme 1. Illustration of sulfonic organosilica nanotubes and hydrolysis of cellobiose.

2. Results and Discussion

2.1. Characterization of Sulfonic Organosilica Nanotubes

Sulfhydryl-functionalized organosilica nanotubes with ethenyl or phenylene groups in the frameworks were synthesized through the co-condensation of ethenyl- or phenylene-bridged organosilane and 3-mercaptopropyltrimethoxysilane (MPTMS) using self-assembly methods, which were denoted as SH_x-Et-SNT or SH_x-Ph-SNT (x means the ratio of MPTMS amounts in the total precursors), respectively. After the treatment with hydrogen peroxide, sulfonic organosilica nanotubes (SO_3H_x-Et-SNT or SO_3H_x-Ph-SNT) could be obtained. Figure 1 shows the TEM images of $SH_{0.1}$-Et-SNT and $SO_3H_{0.1}$-Et-SNT, confirming that functionalized nanotubes before and after SH oxidation possess clear nanotube structure with several hundred nanometers in length. However, $SO_3H_{0.1}$-Et-SNT exhibits some aggregation, which might be ascribed to the interactions among different SO_3H groups. In addition, the inner diameter from TEM images was about 5 nm and it was large enough for the free diffusion of molecules in the channels. TEM images of other mercaptopropyl organosilica nanotubes ($SH_{0.2}$-Et-SNT, $SH_{0.3}$-Et-SNT, $SH_{0.1}$-Ph-SNT, $SH_{0.2}$-Ph-SNT, and $SH_{0.3}$-Ph-SNT) were shown in Figure S1. Except for some breakage of tubes observed when x = 0.3, all composite materials maintained general tubular structures. In contrast, further increasing MPTMS to x = 0.5 would lead to the collapse of nanotubes, which reveals the larger amount of MPTMS in the precursors could

not form nanotubes (Figure S2a). This may be due to the unmatchable hydrolysis and condensation rate between MPTMS with a large amount and phenylene-bridged organosilane, which therefore destroying the self-assembly process. As a comparison, sulfonic pure silica nanotubes without ethenyl or phenylene in the frameworks were also synthesized, which exhibit tube structures in spite of some agglomeration shown in Figure S2b. This also indicated that organic groups in the frameworks could help nanotubes disperse from each other to obtain uniform nanotube structures.

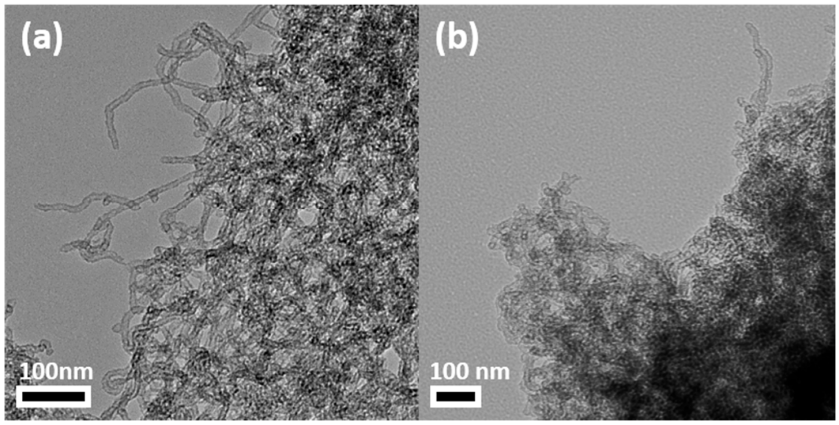

Figure 1. Transmission electron microscopy (TEM) images of (**a**) $SH_{0.1}$-Et-SNT; (**b**) $SO_3H_{0.1}$-Et-SNT.

The nitrogen adsorption-desorption isotherms of all samples before and after SH oxidation were shown in Figures 2, S3 and S4. Typical type IV isotherms with two hysteresis loops, which represent the interior pore and stacking pores among nanotubes except for $SO_3H_{0.5}$-Ph-SNT, could be observed [15,16]. It was found that the Brunauer-Emmett-Teller (BET) surface areas decreased gradually with the sulfur content increasing possibly because of the introduction of mercaptopropyl [17]. Using SH_x-Ph-SNT as examples, when x changed from 0.1, 0.2 to 0.3, the BET surface areas decreased from 834 $m^2 \cdot g^{-1}$, 560 $m^2 \cdot g^{-1}$ to 530 $m^2 \cdot g^{-1}$, respectively. Likewise, pore volume and pore size also declined from 2.1 $cm^2 \cdot g^{-1}$ and 6.5 nm to 1.2 $cm^2 \cdot g^{-1}$ and 5.4 nm, respectively (Table S1). After the SH oxidation (seen in Table 1), a similar trend was found and surface areas declined from 537 $m^2 \cdot g^{-1}$, 485 $m^2 \cdot g^{-1}$ to 421 $m^2 \cdot g^{-1}$ corresponding to x = 0.1, 0.2 and 0.3, while pore sizes stayed the same. Nevertheless, when MPTMS was taken up to 50% in the silica precursors, the hysteresis loop in middle relative pressure can hardly be found (Figure S4), indicating that nanotubes were not formed, which was also confirmed by TEM (Figure S2a). In addition, the BET surface areas were 365 and 231 $m^2 \cdot g^{-1}$ for $SH_{0.5}$-Ph-SNT and $SO_3H_{0.5}$-Ph-SNT, respectively.

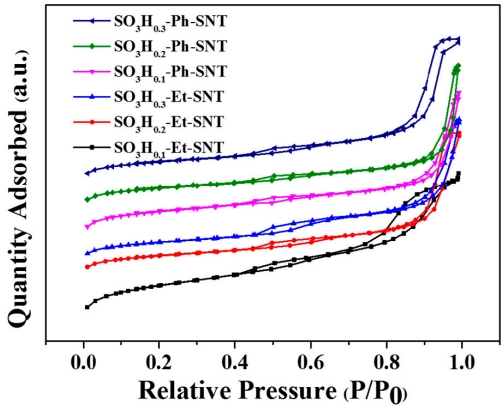

Figure 2. Nitrogen adsorption-desorption isotherms of $SO_3H_{0.1}$-Et-SNT, $SO_3H_{0.2}$-Et-SNT, $SO_3H_{0.3}$-Et-SNT, $SO_3H_{0.1}$-Ph-SNT, $SO_3H_{0.2}$-Ph-SNT, $SO_3H_{0.3}$-Ph-SNT.

Table 1. Physicochemical properties of various catalysts with different sulfur contents and bridged groups.

Samples	BET Surface Area [a] (m^2/g)	Pore Diameter [b] (nm)	Acid Content [c] (mmol/g)	Acid Density [d] ($\mu mol/m^2$)	Oxidation Degree (%) [e]
$SO_3H_{0.1}$-Et-SNT	647	5.5	0.48	0.74	75
$SO_3H_{0.2}$-Et-SNT	562	5.4	0.94	1.67	73
$SO_3H_{0.3}$-Et-SNT	380	5.6	1.66	4.37	66
$SO_3H_{0.1}$-Ph-SNT	537	4.3	0.42	0.78	81
$SO_3H_{0.2}$-Ph-SNT	485	4.8	0.89	1.84	63
$SO_3H_{0.3}$-Ph-SNT	421	4.8	1.41	3.35	77
$SO_3H_{0.5}$-Ph-SNT	231	-	2.02	8.74	-
SO_3H-SNT	544	5.6	0.67	1.23	-

[a] Surface area was determined using the Brunauer-Emmett-Teller (BET) model; [b] Pore size was estimated Barrett-Joyner-Halenda (BJH) method with adsorption branch; [c] Acid content was verified by acid-base titration; [d] Acid density was calculated from acid contents (acid-base titration) divided by BET surface areas; [e] Oxidation degree was determined by XPS characterization.

The contents of acidic active sites are measured through the acid-base titration method. After ion exchange with 2 mol/L KCl solution, H^+ was transferred from solid to the mixture and titrated by 0.01 mol/L sodium hydroxide [18,19]. On the basis of titration, acid contents on surface of $SO_3H_{0.1}$-Et-SNT, $SO_3H_{0.2}$-Et-SNT, $SO_3H_{0.3}$-Et-SNT, $SO_3H_{0.1}$-Ph-SNT, $SO_3H_{0.2}$-Ph-SNT and $SO_3H_{0.3}$-Ph-SNT were 0.48, 0.94, 1.96, 0.42, 0.89 and 1.41 $mmol \cdot g^{-1}$, respectively. The acid densities on the surface could be calculated to 0.74, 1.67 4.37, 0.78, 1.84, 3.35 $\mu mol \cdot m^{-2}$ according to the surface areas of each sample. In order to know if all the –SH groups were oxidized, the X-ray photoelectron spectroscopy (XPS) was used to investigate the oxidation degrees in the solid catalysts. Compared to mercaptopropyl organosilica in which peak at 164 eV assigned to SH groups (Figure S5), a new peak with higher intensity at 169 eV could be detected (Figure 3), corresponding to SO_3H groups after oxidation [20]. However, partial SH also existed after H_2O_2 treatment due to the unexposed SH groups buried in the tube walls [21]. According to the relative ratio of peak areas for SH and SO_3H, the oxidation degree could be computed and the results ranged from 63% to 81% (Table 1).

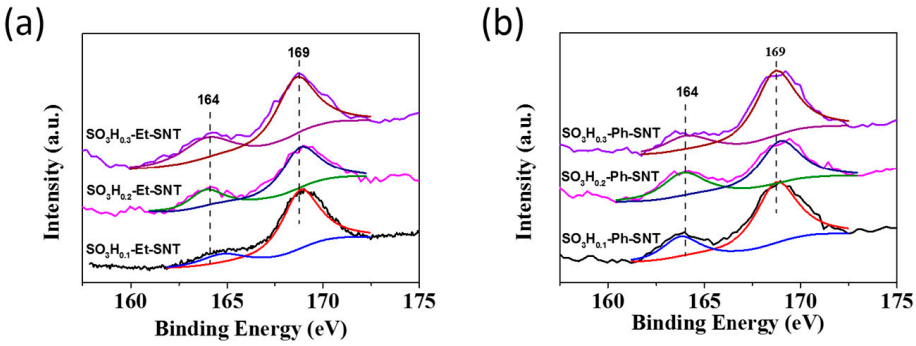

Figure 3. X-ray photoelectron spectroscopy (XPS) of (**a**) SO_3H_x-Et-SNT and (**b**) SO_3H_x-Ph-SNT (x = 0.1, 0.2, 0.3).

In order to further verify the framework compositions of the organic-inorganic hybrid solid acids, the solid-state ^{13}C cross polarization magic-angle spinning (CP MAS) and ^{29}Si magic-angle spinning (MAS) nuclear magnetic resonances (NMR) were conducted using $SO_3H_{0.1}$-Et-SNT and $SO_3H_{0.1}$-Ph-SNT as the samples (Figure 4). In the ^{13}C NMR spectrum of $SO_3H_{0.1}$-Et-SNT (Figure 4a), a remarkable peak at 5 ppm is attributed to the overlap of bridging ethenyl units and C2 carbon species in propyl group. The other two extremely weak peaks at 18 ppm and 55 ppm, also existing in $SO_3H_{0.1}$-Ph-SNT, could be recognized as C1 and C3 carbon species, respectively. The highest resonance signal at around 135 ppm in Figure 4c belongs to the phenylene units while another obvious resonance at about 70 ppm was assigned to the remaining template [19,22,23]. Regarding the ^{29}Si NMR spectrum

(Figure 4b,d), three primary signals at −63 ppm, −71 ppm and −79 ppm can be assigned to T1 [-C_2H_4-Si(OSi)$(OH)_2$], T2 [-C_2H_4-Si$(OSi)_2(OH)$] and T3 [-C_2H_4-Si$(OSi)_3$] Si species, respectively [24,25]. The above results related to NMR imply the formation of an organosilica structure bridged with ethenyl or phenylene and the successful incorporation of mercaptopropyl groups in the frameworks.

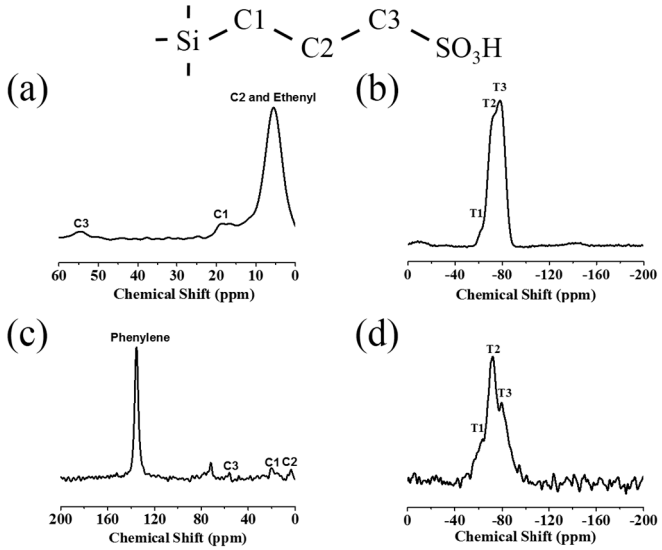

Figure 4. ^{13}C nuclear magnetic resonances (NMR) spectra of (**a**) $SO_3H_{0.1}$-Et-SNT and (**c**) $SO_3H_{0.1}$-Ph-SNT, ^{29}Si NMR spectra of (**b**) $SO_3H_{0.1}$-Et-SNT and (**d**) $SO_3H_{0.1}$-Ph-SNT.

2.2. Hydrolysis of Cellobiose

Organic-inorganic composite catalysts with nanotubes structure, SO_3H_x-Et-SNT and SO_3H_x-Ph-SNT, were expected as efficient catalysts applying in the hydrolysis of cellobiose due to their strong Brønsted acid sites, high acid densities, large specific areas and hollow structures. In all reactions, the mol ratio of acid active sites to substrates was set to 1:14 under the nitrogen pressure of 2.5 MPa at 150 °C.

Figure 5 illustrates time-dependent kinetic curves of SO_3H_x-Et-SNT and SO_3H_x-Ph-SNT as catalysts, respectively, under the same reaction conditions. Although the amount of acids used in the reaction was kept the same, the reaction activities varied from the different acid densities in the frameworks. The conversion of cellobiose for $SO_3H_{0.1}$-Et-SNT and $SO_3H_{0.1}$-Ph-SNT was 65% and 70% within 2 h, respectively (Table 2). With the increasing of MPTMS to 20%, the conversion rose to 73% and 79% with respect to $SO_3H_{0.2}$-Et-SNT and $SO_3H_{0.2}$-Ph-SNT. As to $SO_3H_{0.3}$-Et-SNT and $SO_3H_{0.3}$-Ph-SNT, conversions reached to 87% and 92%, which were the highest among all the catalysts, suggesting that higher acid density is beneficial to the hydrolysis reaction. Apart from high conversions, SO_3H_x-Et-SNT and SO_3H_x-Ph-SNT can give at least 89% glucose selectivity within two hours, which is generally higher than other reported results [26,27]. Figure S6 shows the liquid chromatography spectra of the reactant and product at the different reaction time using $SO_3H_{0.3}$-Ph-SNT as catalyst, indicating that almost no by-products were formed besides glucose.

Nevertheless, when $SO_3H_{0.5}$-Ph-SNT synthesized at the proportion of MTPMS in silane precursors of 50% was used, the conversion of cellobiose could only reach 78% within 2 h (Figure 6). The lower activity of $SO_3H_{0.5}$-Ph-SNT was due to the non-nanotube structure, which was not beneficial to the efficient transport of the reactant or product. In addition, SO_3H_x-Ph-SNT nanotubes always possess a higher conversion compared to SO_3H_x-Et-SNT even with the same acid density. Since phenylene is more hydrophobic than ethenyl as we know, we suppose that the more hydrophobic organic groups in the frameworks may be more suitable for the conversion of cellobiose to glucose. In order to verify the hypothesis, we further synthesized SO_3H-SNT without any organic groups in the frameworks.

Lower conversion (52%) and yield (46%) were obtained when using the same amount of acid under the same reaction conditions, demonstrating that organic components indeed have positive effects on this reaction (Figure 6).

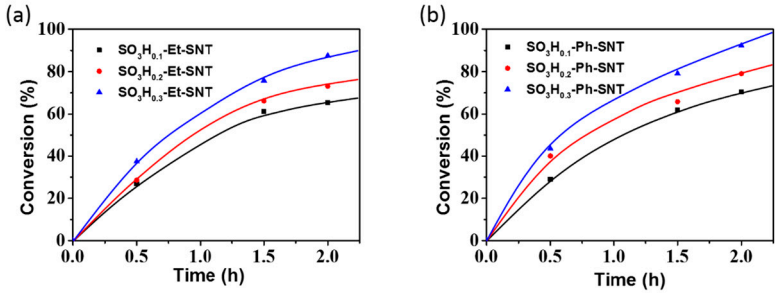

Figure 5. Cellobiose conversion using (**a**) $SO_3H_{0.1}$-Et-SNT, $SO_3H_{0.2}$-Et-SNT, $SO_3H_{0.3}$-Et-SNT and (**b**) $SO_3H_{0.1}$-Ph-SNT, $SO_3H_{0.2}$-Ph-SNT, $SO_3H_{0.3}$-Ph-SNT as catalysts. Reaction conditions: 50 mL autoclave, 20 mL deionized water, 0.2 g cellobiose, the mol ratio of substrates to acid active sites = 14, 150 °C, 2.5 MPa nitrogen, 800 rpm.

Table 2. Catalytic performance of several sulfonic organosilica nanotubes towards hydrolysis of cellobiose [a].

Entry	Catalysts	Conversion of Cellobiose (%) [b]	Selectivity of Glucose (%)	TON [c]	TOF (h^{-1}) [d]
1	$SO_3H_{0.1}$-Et-SNT	65	93	8.4	7.5
2	$SO_3H_{0.2}$-Et-SNT	73	96	9.8	8.0
3	$SO_3H_{0.3}$-Et-SNT	87	89	12.2	10.4
4	$SO_3H_{0.1}$-Ph-SNT	70	90	8.8	8.1
5	$SO_3H_{0.2}$-Ph-SNT	79	92	10.1	11.1
6	$SO_3H_{0.3}$-Ph-SNT	92	96	12.3	12.1
7	$SO_3H_{0.5}$-Ph-SNT	78	91	9.8	7.0
8	SO_3H-SNT	52	88	6.4	7.8

[a] Reaction conditions: 50 mL autoclave, 20 mL deionized water, 0.2 g cellobiose, substrates: acid active sites = 14, 150 °C, 2.5 MPa Nitrogen, 800 rpm; [b] The conversion was obtained within 2 h; [c] TON = the conversion × the selectivity/the amount of catalyst; [d] TOF was calculated from the initial reaction rate by using the conversion of cellobiose at 0.5 h.

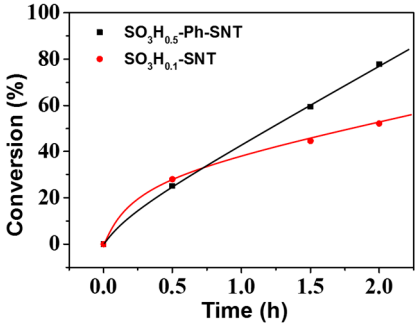

Figure 6. Cellubiose conversion using $SO_3H_{0.5}$-Ph-SNT and SO_3H-SNT as catalysts. Reaction conditions: 50 mL autoclave, 20 mL deionized water, 0.2 g cellubiose, substrates: acid active sites = 14, 150 °C, 2.5 MPa nitrogen, 800 rpm.

More interestingly, a relationship between turnover frequency (TOF) and acid density could be found in Figure 7. Under the same reaction conditions, TOF increased to 12.1 h^{-1} from 8.1 h^{-1} when the acid density was changed to 3.35 from 0.78 μmol·m^{-2} for SO_3H_x-Ph-SNT, which suggests that the synergetic effect among acid sites might existed. Yang's group reported the synergetic effect among

SO_3H groups and they speculated that formation of H-bond interactions derived from closer acid sites would enhance acid strength, therefore increasing the cooperation effect [28].

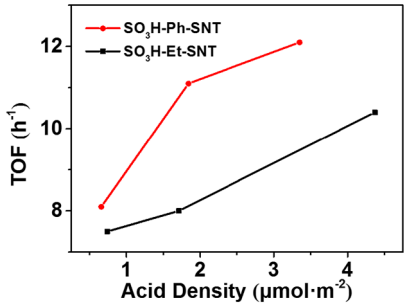

Figure 7. Relationship between turnover frequency (TOF) and acid density for SO_3H_x-Ph-SNT and SO_3H_x-Et-SNT.

The reusability of the acid catalysts was investigated using $SO_3H_{0.3}$-Ph-SNT as catalysts and the results are showed in Figure 8. Although the conversion of cellobiose and the yield of glucose decreased to 83% and 75% for the second run, it still exhibited good performance for the sixth reuse with the conversion of 66% and the yield of 59%. After the reaction, we investigated the sulfur leaching in the solution. According to the data from ICP-MS, around 30% sulfur leached during the reaction, which might lead to the decreased activity during the recycling. However, the leaching amount was somewhat lower than those of other catalysts systems reported [29]. The reason for this might be the existence of organic groups in the frameworks, which could bear the harsh conditions during the hydrolysis reaction.

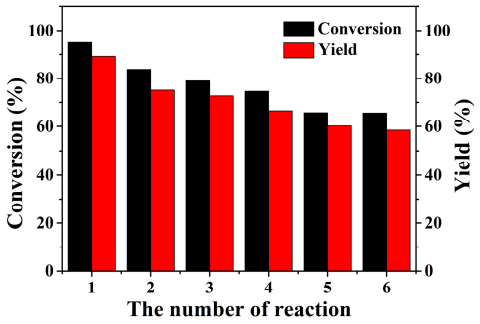

Figure 8. Reusability of $SO_3H_{0.3}$-Ph-SNT. Reaction conditions: 50 mL autoclave, 20 mL deionized water, 0.2 g cellobiose, substrates: acid active sites = 14, 150 °C, 2.5 MPa nitrogen, 800 rpm, 2 h.

In order to investigate reaction temperature effect on this system, reactions using $SO_3H_{0.1}$-Ph-SNT as catalysts at different temperatures were carried out and the results were shown in Figure S7. At 130 °C, both conversion and yield were lower than 40%, even though the selectivity was close to 100%. The gap between the conversion and the yield was widened gradually with the increasing of the temperature, indicating that higher reaction temperature has an adverse impact on glucose selectivity. At 160 °C, the conversion reached nearly 100% and the selectivity of glucose was 88% within 2 h.

3. Materials and Methods

3.1. Chemicals and Regents

1,2-bis(trimethoxysilyl)ethane (BTME), 1,4-bis(triethoxysilyl)benzene (BTEB), 3-mercaptopropy ltrimethoxysilane (MPTMS), tetraethyl orthosilicate (TEOS) and potassium chloride were purchased from J&K Scientific Ltd., Beijing, China. Hydrochloric acid (37%), sulfuric acid (98%) and ethanol were

obtained from Real&Lead Chemical Co. Ltd., Tianjin, China. Hydrogen peroxide (40%), cellobiose and Pluronic P123 were received from Sigma-Aldrich, St. Louis, MO, USA. All reagents were used without further purification. Chromatogram analysis was carried out on N2000 chromatographic work station, Version 3.20, Zhejiang University, Hangzhou, China.

3.2. Catalyst Preparation

3.2.1. Synthesis of Sulfonic Ethyl-Bridged Organosilica Nanotubes

According to our previous work [10] and a method reported by Wang [18], sulfonic organosilica nanotubes bridged with ethenyl in the framework were synthesized as follows: Typically, a certain amount of BTME was added dropwise into 135 mL of hydrochloric acid (2 mol/L) containing 1.75 g of potassium chloride and 0.55 g of P123 with vigorous stirring at 38 °C. The mixture was kept static for 12 h before the addition of MPTMS. The total precursor amounts based on Si were 7 mmol and MPTMS was adjusted to 10%, 20%, 30% and 50%, respectively. After being stirred for 24 h, the mixture was subsequently transferred to a BTFE bottle and aged at 100 °C for 24 h under static conditions. The product was collected by filtration, washed by deionized water and dried at room temperature. Surfactants were removed by extraction in ethanol and HCl under refluxing. The obtained samples were named as SH_x-Et-SNT (x means the ratio of MPTMS amounts in the total precursors, Et stands for ethenyl groups in the frameworks and SNT is the abbreviation of silica nanotubes).

In order to oxidize SH to SO_3H, 0.5 g of SH_x-Et-SNT was mixed with 20 mL of H_2O_2 (30%) under stirring for 12 h at room temperature, following the treatment of 200 mL H_2SO_4 (0.1 M) for another 12 h. Finally, the suspension was filtered and continually washed by deionized water until the filtrate was neutral. The solids were denoted as SO_3H_x-Et-SNT.

3.2.2. Synthesis of Sulfonic Phenyl-Bridged Organosilica Nanotubes

The synthesis process of SH-Ph-SNT and SO_3H_x-Ph-SNT (Ph stands for phenylene groups in the frameworks) was similar with that of SH-Et-SNT and SO_3H_x-Et-SNT with minor changes. After complete dissolution of 0.275 g of P123 and 0.875 g of KCl in 90 mL of hydrochloric acid (2 mol/L), BTEB was added into the solution drop by drop. Then the solution was continually stirred for 12 h followed by addition of MPTMS. The precursor amounts and the procedures including hydrothermal treatment, extraction of surfactants and SH oxidation were the same as those of SO_3H_x-Et-SNT.

3.2.3. Synthesis of Sulfonic Silica Nanotubes

The synthesis of sulfonic silica nanotubes followed the procedure reported by Yang with a minor revision [30]. Typically, 0.4 g of P123 and 12 g of boric acid were completely dissolved in 160 mL of deionized water with stirring at 40 °C. After that, 1.8 mL of TEOS was dropped into the solution and kept stirring for 12 h followed by addition of 0.2 mL of MPTMS. Then, the mixture was continually stirred at 40 °C for 80 h with gentle stirring and subsequently transferred to a PTFE bottle to be aged at 100 °C for 24 h. Then the mixture was undertaken the same progress with SO_3H_x-Et-SNT, including the template extraction and SH oxidation. The obtained material with pure silica frameworks was named as SH-SNT and SO_3H-SNT, respectively, before and after SH oxidation.

3.3. Characterization

The transmission electron microscopy (TEM) images were taken on a FEI Tecnai G2 F20 electron microscope operated at an acceleration voltage of 200 kV. The nitrogen adsorption-desorption isotherms were measured on Tristar 3000 (Micrometrics) after the samples were outgassed at 120 °C for 3 h. The Brunauer-Emmett-Teller (BET) specific surface areas were calculated using adsorption data at the relative pressure range of P/P_0 = 0.05–0.25. Pore size distributions were calculated from adsorption branch using the Barrett-Joyner-Halenda (BJH) method. Sulfur content in hybrid catalysts was performed on an Elementar Vario Micro cube elemental analyzer (CHNS mode), Lyon, France. ^{13}C and

^{29}Si cross polarization-magic angle spinning nuclear magnetic resonance (CP-MAS NMR) spectra were recorded on a Varian Infinityplus 300 spectrometer, Pale Alto, CA, USA. X-ray photoelectron spectroscopy (XPS) was acquired using a PHI1600 X-ray photoelectron spectroscopy (Perkin Elmer, Waltham, MA, USA). Sulfur leaching when was determined by an Agilent 7700x inductively coupled plasma mass spectrometer (ICP-MS), Santa Clara, CA, USA.

3.4. Catalytic Test

Hydrolysis of cellobiose was carried out in a steal autoclave equipped with a magnetic stirrer. Typically, 0.20 g of cellobiose, a certain amount of catalysts (substrates: active sites = 14) and 20 mL deionized water were added into an autoclave in order. Then, the sealed system was flushed with nitrogen at least 3 times to remove air and finally pressurized to 2.5 MPa. The reactions were carried out at 150 °C for 30 min, 90 min and 120 min, respectively, with magnetic stirring at 800 r/min. To stop the reaction, an icy cold atmosphere was required and after that, the solid catalysts were separated by centrifugation. Liquid phase mixture was analyzed by high performance liquid chromatography (HPLC) equipped with an ICSep ICE-Coregel 87H3 column and a RID detector. The HPLC column was retained at 38 °C, using H_2SO_4 solution (5 mmol/L, 0.6 mL/min) as the mobile phase. Conversions and yields were calculated through calibration curves obtained from external standards method and the equations are showed as blow:

$$Conversion = \frac{\frac{0.2}{342.3} - Cellobiose\ moles\ (detected\ by\ HPLC)}{0.2/342.3} \times 100\% \quad (1)$$

$$Yield = \frac{Glucose\ moles\ (detected\ by\ HPLC)/2}{0.2/342.3} \times 100\% \quad (2)$$

$$Selectivity = \frac{Yield}{Conversion} \times 100\% \quad (3)$$

4. Conclusions

Ethenyl- or phenylene-bridged sulfonic organosilica nanotubes with different acid contents were synthesized through the –SH oxidation of sulfhydryl organosilica nanotubes, which were prepared through an easy soft-template method. The samples exhibited obvious hollow tube structures with pore diameters of about 5 nm evidenced by TEM images and nitrogen adsorption-desorption isotherms. XPS showed about 63% to 81% of –SH groups in the solids were oxidized to –SO_3H and acid contents were ascertained by acid-base titration method. The novel solid acid catalysts exhibited excellent activities in the hydrolysis of cellobiose with the highest conversion of 92% and glucose selectivity of 96% for $SO_3H_{0.3}$-Ph-SNT. Both surface acid densities and organic groups in the nanotube frameworks play important roles on this reaction. Furthermore, the catalysts could be reused at least six times and still showed high activities with the conversion of 66% and the glucose selectivity of 92%. This study provides a new series of sulfonic organosilica nanotubes with different acid densities for the hydrolysis of cellobiose, which have not been reported before.

Supplementary Materials: The following are available online at www.mdpi.com/2073-4344/7/5/127/s1, Figure S1: TEM images of (a) $SH_{0.2}$-Et-SNT, (b) $SH_{0.3}$-Et-SNT, (c) $SH_{0.1}$-Ph-SNT, (d) $SH_{0.2}$-Ph-SNT and (e) $SH_{0.3}$-Ph-SNT, Figure S2: TEM images of (a) $SH_{0.5}$-Ph-SNT and (b) SH-SNT, Figure S3: Nitrogen adsorption-desorption isotherms of $SH_{0.1}$-Et-SNT, $SH_{0.2}$-Et-SNT, $SH_{0.3}$-Et-SNT, $SH_{0.1}$-Ph-SNT, $SH_{0.2}$-Ph-SNT and $SH_{0.3}$-Ph-SNT, Figure S4: Nitrogen adsorption isotherms of SH-SNT, SO_3H-SNT, $SH_{0.5}$-Ph-SNT and $SO_3H_{0.5}$-Ph-SNT, Figure S5: XPS spectrum of $SH_{0.1}$-Et-SNT, Figure S6: Liquid chromatography spectra of mixture including cellubiose (green square) and glucose (orange circle) after reaction using $SO_3H_{0.3}$-Ph-SNT as catalyst, Figure S7: Hydrolysis of cellubiose by using $SO_3H_{0.1}$-Ph-SNT as catalysts at 130 °C, 140 °C, 150 °C and 160 °C, respectively. Reaction conditions: 50 mL autoclave, 20 mL deionized water, substrates: acid active sites = 14, 0.2 g cellubiose, 2.5 MPa Nitrogen, 800 rpm, 2 h. Table S1: Physicochemical properties of SH_x-Et-SNT and SH_x-Ph-SNT.

Acknowledgments: We acknowledge the National Natural Science Foundation of China (No. 21276191, U1662109), the Specialized Research Fund for the Doctoral Program of Higher Education of China (No. 20120032120083), and the Natural Science Foundation of Tianjin, China (No. 16JCQNJC06200) for financial support.

Author Contributions: X.L. and S.R. conceived and designed the experiments; J.S. performed the experiments and analyzed the data; X.Z., H.W. and J.H. contributed analysis tools while J.S. and X.L. wrote the manuscript.

Conflicts of Interest: The authors declare no conflict of interest.

References

1. Alonso, D.M.; Wettstein, S.G.; Dumesic, J.A. Bimetallic catalysts for upgrading of biomass to fuels and chemicals. *Chem. Soc. Rev.* **2012**, *41*, 8075–8098. [CrossRef] [PubMed]
2. Huber, G.W.; Iborra, S.; Corma, A. Synthesis of transportation fuels from biomass: Chemistry, catalysts, and engineering. *Chem. Rev.* **2006**, *106*, 4044–4098. [CrossRef] [PubMed]
3. Huang, Y.-B.; Fu, Y. Hydrolysis of cellulose to glucose by solid acid catalysts. *Green Chem.* **2013**, *15*, 1095–1111. [CrossRef]
4. Salesch, T.; Bachmann, S.; Brugger, S.; Rabelo-Schaefer, R.; Albert, K.; Steinbrecher, S.; Plies, E.; Mehdi, A.; Reyé, C.; Corriu, R.J.P.; et al. New inorganic ± organic hybrid materials for HPLC separationobtained by direct synthesis in the presence of a surfactant. *Adv. Funct. Mater.* **2002**, *12*, 134–142. [CrossRef]
5. Melero, J.A.; van Grieken, R.; Morales, G. Advances in the synthesis and catalytic applications of organosulfonic-functionalized mesostructured materials. *Chem. Rev.* **2006**, *106*, 3790–3812. [CrossRef] [PubMed]
6. Corma, A.; Iborra, S.; Velty, A. Chemical routes for the transformation of biomass into chemicals. *Chem. Rev.* **2007**, *107*, 2411–2502. [CrossRef] [PubMed]
7. Van der Voort, P.; Esquivel, D.; de Canck, E.; Goethals, F.; van Driessche, I.; Romero-Salguero, F.J. Periodic mesoporous organosilicas: From simple to complex bridges; a comprehensive overview of functions, morphologies and applications. *Chem. Soc. Rev.* **2013**, *42*, 3913–3955. [CrossRef] [PubMed]
8. López, M.I.; Esquivel, D.; Jiménez-Sanchidrián, C.; Romero-Salguero, F.J.; van der Voort, P. A "one-step" sulfonic acid PMO as a recyclable acid catalyst. *J. Catal.* **2015**, *326*, 139–148. [CrossRef]
9. Zhang, X.; Su, F.; Song, D.; An, S.; Lu, B.; Guo, Y. Preparation of efficient and recoverable organosulfonic acid functionalized alkyl-bridged organosilica nanotubes for esterification and transesterification. *Appl. Catal. B Environ.* **2015**, *163*, 50–62. [CrossRef]
10. Liu, X.; Li, X.; Guan, Z.; Liu, J.; Zhao, J.; Yang, Y.; Yang, Q. Organosilica nanotubes: Large-scale synthesis and encapsulation of metal nanoparticles. *Chem. Commun. Camb.* **2011**, *47*, 8073–8075. [CrossRef] [PubMed]
11. Song, D.; An, S.; Sun, Y.; Zhang, P.; Guo, Y.; Zhou, D. Ethane-bridged organosilica nanotubes functionalized with arenesulfonic acid and phenyl groups for the efficient conversion of levulinic acid or furfuryl alcohol to ethyl levulinate. *ChemCatChem* **2016**, *8*, 2037–2048. [CrossRef]
12. Liu, X.; Maegawa, Y.; Goto, Y.; Hara, K.; Inagaki, S. Heterogeneous catalysis for water oxidation by an iridium complex immobilized on bipyridine-periodic mesoporous organosilica. *Angew. Chem. Int. Ed. Engl.* **2016**, *55*, 7943–7947. [CrossRef] [PubMed]
13. Long, Y.-Z.; Li, M.-M.; Gu, C.; Wan, M.; Duvail, J.-L.; Liu, Z.; Fan, Z. Recent advances in synthesis, physical properties and applications of conducting polymer nanotubes and nanofibers. *Prog. Polym. Sci.* **2011**, *36*, 1415–1442. [CrossRef]
14. Su, D.S.; Perathoner, S.; Centi, G. Nanocarbons for the development of advanced catalysts. *Chem. Rev.* **2013**, *113*, 5782–5816. [CrossRef] [PubMed]
15. Song, D.; An, S.; Sun, Y.; Guo, Y. Efficient conversion of levulinic acid or furfuryl alcohol into alkyl levulinates catalyzed by heteropoly acid and ZrO_2 bifunctionalized organosilica nanotubes. *J. Catal.* **2016**, *333*, 184–199. [CrossRef]
16. Mandal, M.; Kruk, M. Family of single-micelle-templated organosilica hollow nanospheres and nanotubes synthesized through adjustment of organosilica/surgactant ratio. *Chem. Mater.* **2011**, *24*, 123–132. [CrossRef]
17. Lim, M.H.; Stein, A. Comparative studies of grafting and direct syntheses of inorganic-organic hybrid mesoporous materials. *Chem. Mater.* **1999**, *11*, 3285–3295. [CrossRef]

18. Wang, P.; Bai, S.; Zhao, J.; Su, P.; Yang, Q.; Li, C. Bifunctionalized hollow nanospheres for the one-pot synthesis of methyl isobutyl ketone from acetone. *ChemSusChem* **2012**, *5*, 2390–2396. [CrossRef] [PubMed]
19. Lu, B.; An, S.; Song, D.; Su, F.; Yang, X.; Guo, Y. Design of organosulfonic acid functionalized organosilica hollow nanospheres for efficient conversion of furfural alcohol to ethyl levulinate. *Green Chem.* **2015**, *17*, 1767–1778. [CrossRef]
20. Russo, P.A.; Antunes, M.M.; Neves, P.; Wiper, P.V.; Fazio, E.; Neri, F.; Barreca, F.; Mafra, L.; Pillinger, M.; Pinna, N.; et al. Solid acids with SO_3H groups and tunable surface properties: Versatile catalysts for biomass conversion. *J. Mater. Chem. A* **2014**, *2*, 11813–11824. [CrossRef]
21. Hamoudi, S.; Kaliaguine, S. Sulfonic acid-functionalized periodic mesoporous organosilica. *Microporous Mesoporous Mater.* **2003**, *59*, 195–204. [CrossRef]
22. Rác, B.; Hegyes, P.; Forgo, P.; Molnár, Á. Sulfonic acid-functionalized phenylene-bridged periodic mesoporous organosilicas as catalyst materials. *Appl. Catal. A Gen.* **2006**, *299*, 193–201. [CrossRef]
23. Zhang, L.; Liu, J.; Yang, J.; Yang, Q.; Li, C. Direct synthesis of highly ordered amine-functionalized mesoporous ethane-silica. *Microporous Mesoporous Mater.* **2008**, *109*, 172–183. [CrossRef]
24. Huang, J.; Zhang, F. Periodic mesoporous organosilica grafted palladium organometallic complex: Efficient heterogeneous catalyst for water-medium organic reactions. *Appl. Organomet. Chem.* **2010**, *24*, 767–773. [CrossRef]
25. Wei, L.; Shi, D.; Zhou, Z.; Ye, P.; Wang, J.; Zhao, J.; Liu, L.; Chen, C.; Zhang, Y. Functionalized self-assembled monolayers on mesoporous silica nanoparticles with high surface coverage. *Nanoscale Res. Lett.* **2012**, *7*, 334. [CrossRef] [PubMed]
26. Delidovich, I.; Palkovits, R. Impacts of acidity and textural properties of oxidized carbon materials on their catalytic activity for hydrolysis of cellobiose. *Microporous Mesoporous Mater.* **2016**, *219*, 317–321. [CrossRef]
27. Fukuhara, K.; Nakajima, K.; Kitano, M.; Hayashi, S.; Hara, M. Synthesis and acid catalysis of zeolite-templated microporous carbons with SO_3H groups. *Phys. Chem. Chem. Phys.* **2013**, *15*, 9343–9350. [CrossRef] [PubMed]
28. Zhang, X.; Zhao, Y.; Xu, S.; Yang, Y.; Liu, J.; Wei, Y.; Yang, Q. Polystyrene sulphonic acid resins with enhanced acid strength via macromolecular self-assembly within confined nanospace. *Nat. Commun.* **2014**, *5*, 3170. [CrossRef] [PubMed]
29. Karaki, M.; Karout, A.; Toufaily, J.; Rataboul, F.; Essayem, N.; Lebeau, B. Synthesis and characterization of acidic ordered mesoporous organosilica SBA-15: Application to the hydrolysis of cellobiose and insight into the stability of the acidic functions. *J. Catal.* **2013**, *305*, 204–216. [CrossRef]
30. Yang, J.; Chen, W.; Ran, X.; Wang, W.; Fan, J.; Zhang, W.-X. Boric acid assisted formation of mesostructured silica: From hollow spheres to hierarchical assembly. *RSC Adv.* **2014**, *4*, 20069–20076. [CrossRef]